


## Another exact ground state of a two-dimensional quantum antiferromagnet

Pratyay Ghosh , Tobias Müller , and Ronny Thomale 

*Institut für Theoretische Physik und Würzburg-Dresden Cluster of Excellence ct.qmat, Universität Würzburg, Am Hubland Campus Süd, Würzburg 97074, Germany*

 (Received 14 December 2021; revised 23 February 2022; accepted 9 May 2022; published 24 May 2022)

We present the exact dimer ground state of a quantum antiferromagnet on the maple-leaf lattice. A coupling anisotropy for one of the three inequivalent nearest-neighbor bonds is sufficient to stabilize the dimer state. Together with the Shastry-Sutherland Hamiltonian, we show that this is the only other model with an exact dimer ground state for all two-dimensional lattices with uniform tilings.

DOI: [10.1103/PhysRevB.105.L180412](https://doi.org/10.1103/PhysRevB.105.L180412)

**Introduction.** For decades, quantum antiferromagnets have been at the center of condensed matter research [1–3]. Frustrated magnetic couplings, combined with the noncommutativity of quantum spin operators, make it a challenging task to identify models which allow for an analytical understanding of their ground states. In particular, this applies to spatial dimensions greater than one, where integrability is more elusive, the Bethe ansatz, in general, does not apply, and conformal symmetry does not generate an extensive amount of conserved operators.

A first pivotal step in this direction was reached by Shastry and Sutherland in 1981 [4] where, in continuation of a spin chain model by Majumdar and Ghosh [5], the first quantum antiferromagnet with uniform tilings was found to exhibit an exact dimer ground state. While a significant fraction of the research activity subsequently shifted to topologically ordered exact ground states of quantum antiferromagnets such as chiral spin liquids [6,7], valence bond liquids [8,9], or the  $Z_2$  spin liquid realized in the Kitaev model [10–12], the Shastry-Sutherland model (SSM) has prevailed as an important crystallization point for discoveries and theoretical developments in quantum antiferromagnets.

In this Letter, we propose a spin model defined on the maple-leaf lattice. The maple-leaf tiling is called snub trihexagonal tiling ( $p6$  space group), where four triangles and one hexagon surround each site of the lattice (Fig. 1). This corresponds to a  $1/7$ -site ( $1/6$ -bond) depleted version of the triangular lattice with coordination number 5 [13]. We find that the phase diagram of our model hosts an exact dimer ground state, and show that our Hamiltonian, aside from the SSM, is the only other such two-dimensional (2D) model with uniform tilings.

**Model.** Our Hamiltonian is given by

$$\mathcal{H} = \sum_{\langle kl \rangle} h_{kl} + \sum_{\langle km \rangle} h_{km} + 2\alpha \sum_{\langle lm \rangle} h_{lm} + B \sum_i S_i^z. \quad (1)$$

Aside from a Zeeman term, there are separate summations over the three inequivalent nearest-neighbor bonds  $kl$ ,  $km$ , and  $lm$  on the maple-leaf lattice denoted blue (dashed), red

(dotted), and green (double line), respectively (Fig. 1).  $h_{ij}$  represents the XXZ-type spin exchange interaction ( $J_z, J_\perp > 0$ )

$$h_{ij} = J_z S_i^z S_j^z + J_\perp (S_i^x S_j^x + S_i^y S_j^y) \quad (2)$$

between the sites  $i$  and  $j$ , where  $S_i^\mu$  denotes the  $\mu = x, y, z$  component of the  $\mathfrak{su}(2)$  spin operator acting on the spin- $S$  representation on site  $i$ . We label (1) as the maple-leaf model (MLM). The Heisenberg model on the maple-leaf lattice has been studied previously [14–17], where the exact dimer state is argued to be an eigenstate [14] and some numerical indication of a pronounced dimerization propensity has been found [16].

**Ground state analysis.** To achieve an exact solution of the MLM, we first rewrite the bond summations in (1) as the sum over interacting spins on triangles

$$\mathcal{H} = \sum (\text{triangle}_1 + \text{triangle}_2 + \text{triangle}_3 + \text{triangle}_4 + \text{triangle}_5 + \text{triangle}_6). \quad (3)$$

For this, we have split the interaction  $2\alpha h_{lm}$  on the double green bonds in Fig. 1 to construct two adjacent triangles sharing this bond. These triangles are formed by pairwise differently colored bond interactions

$$h_\Delta = h_{kl} + h_{km} + \alpha h_{lm} + \frac{B}{2} (S_i^z + S_m^z). \quad (4)$$

From the triangular decomposition, (1) turns out to be a frustration-free model [4,5,18,19], in the sense that the ground state minimizes the energy of each  $h_\Delta$  individually. Note that if there are  $N$  sites for the maple-leaf lattice, there are  $N$  such tricolored triangles and therefore  $N/2$  green bonds.

For large  $\alpha$ , the ground state of a single tricolored triangle is a singlet of the spins forming the green bond, which is strongest among the three types of nearest-neighbor bonds, denoted by  $|lm\rangle$ . Moreover,  $(h_{kl} + h_{km})|lm\rangle = 0$ , leading to the first two terms in (4) not to contribute to the energy of the triangle. We construct the tensor product state

$$|\psi\rangle = \bigotimes_{\langle lm \rangle} |lm\rangle, \quad (5)$$

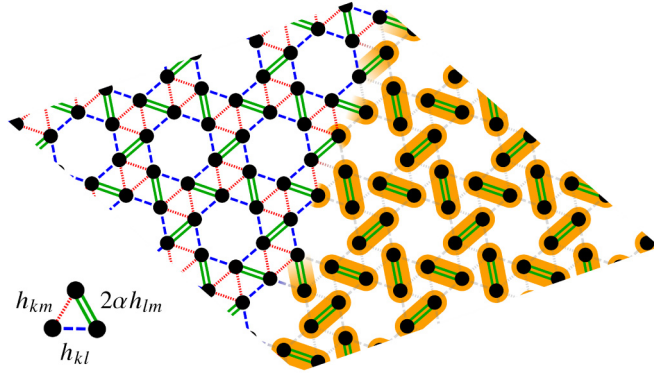


FIG. 1. Maple-leaf lattice (left) and the dimer eigenstate of the Hamiltonian in (1) (right). According to (1) there are three inequivalent nearest-neighbor couplings denoted red (dotted), blue (dashed), and green (double line). The singlets (yellow ellipses) reside on the green bonds. As the red and blue couplings do not contribute to the energy, it is an eigenstate of (1).

which covers the entire spin lattice (see Fig. 1). The first two terms of (1) do not renormalize  $|\psi\rangle$ , thus making (5) an exact eigenstate of the MLM. The corresponding energy density, which is solely determined by the interactions on the green bonds, is given by

$$E/N = -\alpha \frac{S(S+1)}{3} (J_z + 2J_\perp). \quad (6)$$

From the variational principle, if  $e_\Delta$  is the ground state energy of the individual triangles (4), then (6) serves as an upper bound for the ground state energy density of the system, i.e.,  $E_0/N \geq e_\Delta$ . The equality  $E_0/N = e_\Delta$  should hold when  $\alpha$  is greater than a lower bound  $\alpha_{b1}$ , where the dimer state  $|\psi\rangle$  becomes the exact ground state of the MLM. For spin- $\frac{1}{2}$ , this

bound is given by  $\alpha_{b1} = \frac{(B+J_z) + \sqrt{(B+J_z)^2 + 4J_\perp(J_z+J_\perp)}}{2(J_z+J_\perp)}$ , and can likewise be obtained for other spin- $S$  representations [20]. Note that while (5) ceases to be the ground state of the MLM for  $\alpha < \alpha_{b1}$  from a variational principle, it might still be the exact ground state. In any case, (5) still is an exact eigenstate of the MLM, bearing some similarity to the motif of scar states in the context of many-body localization [21].

In order to allow for an exact dimer ground state in accordance with the triangle decomposition explained above, any model needs to satisfy two conditions: (i) Every bond must be part of a triangle where at least one bond is symmetry inequivalent and (ii) this bond must be shared between two triangles. For MLM, the green bonds are not related by symmetry to the other bonds, which satisfies (i), and are shared between two triangles, which satisfies (ii). Note that, to meet (i), we intentionally avoid a triangle decomposition involving red bond only triangles, but arrange them in three tricolored triangles accordingly. Further analyzing the geometric restrictions of uniformly tiling Euclidean space [22,23], the exact dimer state construction above confines us to the lattices with coordination number 5 made with the tiles of vertex configuration 3.3.3.3.6 or 3.3.4.3.4, where the sequence of numbers represents the number of sides of the faces around the vertex [20]. The 1-uniform tilings of the former generate the maple-leaf lattice, while the latter yields the Shastry-Sutherland model

(SSM), where the existence of an exact dimer state was first found [4]. These two tiles can also produce other lattices with  $k$ -uniform tilings for  $k \geq 2$ , but either condition (i) or (ii) is violated in all those cases. Thus, the MLM and SSM exhaust the list of all uniform 2D lattices that can host an exact dimer state (5). Except for MLM and SSM, any alternative 2D model with an exact dimer state is either defined on a lattice with nonuniform tilings or includes further neighbor couplings [24,25]. For the remainder part of this Letter where we focus on the analysis of the coupling anisotropy  $\alpha$  in the MLM, we confine ourselves to (1) with  $J_z = J_\perp = 1$  and  $B = 0$ .

*Classical limit.* Setting  $S \rightarrow \infty$  [26,27], the MLM for  $\alpha \leq 1$  yields local  $120^\circ$  order on individual red triangles, with a nonlocal spin canting induced by the blue and the green bonds [15,16,28], which we denote as *canted*  $120^\circ$  (c $120^\circ$ ) order in the following. The energy is given by

$$E_c/N = -\frac{1}{2} + \cos(\Phi) + \alpha \sin\left(\Phi - \frac{\pi}{6}\right), \quad (7)$$

where  $\Phi = \pi - \cos^{-1}\left(\frac{2-\alpha}{2\sqrt{\alpha^2-\alpha+1}}\right)$  parametrizes the canting between spins across the blue bonds (Fig. 2).

The canting can be reconciled from the limit  $\alpha = 0$ , where the frustrated red triangles will assume a  $120^\circ$  order, while blue bonds only provide antiparallel orientation of neighboring spins without introducing any additional frustration. For  $\alpha > 0$ , the green bonds start to contest the antiferromagnetic ordering on the blue bonds, introducing the canting between neighboring spins on different red triangles. In the particular case of  $\alpha = 1$ , the MLM produces a uniform  $120^\circ$  order akin to the Heisenberg antiferromagnet on a triangular lattice. Similar to the exact dimer ground state analysis above, one can understand this as one splits the green bonds, leading to isolated triangular motifs of three tricolored triangles, where the equality of all bond couplings establishes the uniform  $120^\circ$  order. For  $\alpha > 1$ , aside from the trivial decoupled dimer state limit for  $\alpha \rightarrow \infty$ , a large- $N$  analysis [29] ceases to give a unique ground state. There, as one effectively removes the spin normalization constraint, we find a subextensive degeneracy of ground states [20]. In contrast to the c $120^\circ$

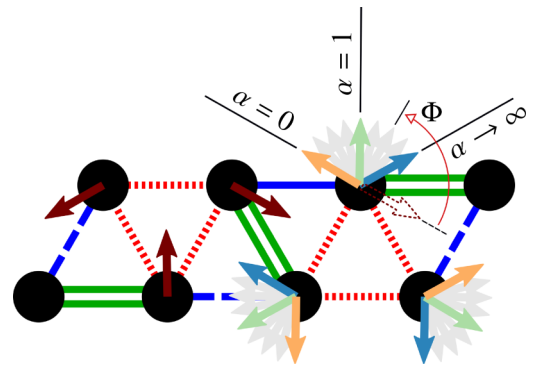


FIG. 2. Canted  $120^\circ$  order: Spins on red triangles (brown) show  $120^\circ$  order, while those connected by blue bonds are canted by an angle  $\Phi(\alpha)$ . As a function of  $\alpha$ , spins across blue bonds are antiparallel for  $\alpha = 0$  (orange), uniform  $120^\circ$  order appears for  $\alpha = 1$  (light green), and decoupled green dimer bonds are formed for  $\alpha \rightarrow \infty$  (light blue).

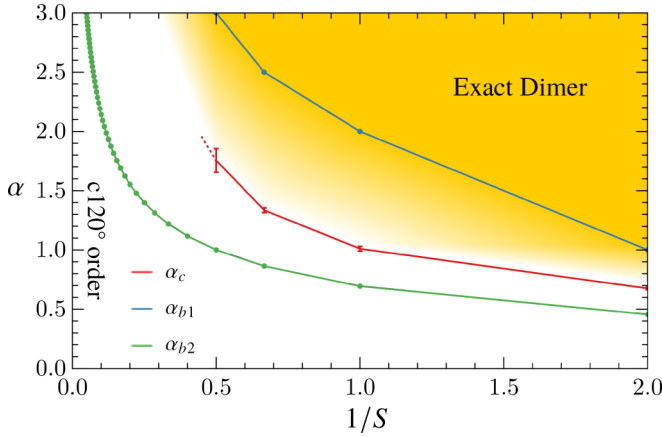


FIG. 3. Dimer phase diagram of MLM as a function of bond coupling  $\alpha$  and spin  $S$ .  $\alpha_{b1}$  denotes a lower bound above which the MLM is exactly solvable.  $\alpha_{b2}$  is an upper bound of  $\alpha$  below which  $c120^\circ$  serves as a better lower bound of energy than (6).  $\alpha_c$  is the numerically obtained critical value of  $\alpha$  above which (5) stabilizes.

state for  $\alpha < 1$ , this manifold cannot form a normalized spin state. In accordance with earlier studies [16], for normalized spins, we do not find any lower-energy state than the  $c120^\circ$  state.

The particular source of frustration in the MLM plays a pivotal role in preventing the system from achieving a global energy minimum by simultaneously minimizing the individual local energies of the tricolored triangles, and thereby forbids, apart from the special point  $\alpha = 1$ , the stabilization of a commensurate magnetic ordering. Instead, our observed canted  $120^\circ$  order bears similarities to frustration-driven *block-spiral magnetism* found in one-dimensional strongly interacting itinerant fermion models away from half filling (see Ref. [30] and references therein), with  $120^\circ$ -ordered triangles spiraling with an  $\alpha$ -dependent pitch. To our knowledge, the MLM is the only example where such a state is realized in either two spatial dimensions or within a local spin model.

*Dimer phase diagram.* Together with  $\alpha_{b1}$  from the exact dimer ground state analysis, we complement our analysis of the MLM through a density matrix renormalization group (DMRG) study in order to obtain an estimate of the critical  $\alpha_c$ , such that for  $\alpha \geq \alpha_c$ , (5) is the exact ground state. The DMRG calculations are performed on a 108-site cluster [20] using the ITENSOR library [31]. Combined, the dimer phase diagram of the MLM is presented in Fig. 3, where we only show those results for different values of  $S$  where the DMRG results are converged. As expected,  $\alpha_c$  turns out to be smaller than  $\alpha_{b1}$  which takes the values 1 for  $S = 1/2$  and  $1 + S$  for  $S \geq 1$ . Even though this is beyond the numerical range of investigation, we expect  $\alpha_c$  to converge asymptotically against  $\alpha_{b1}$  for increasing  $S$ . For the sake of an additional consistency check, we evaluate  $\alpha_{b2}$  below which the  $c120^\circ$  state serves as a better lower bound for the energy than the dimer state (5), by comparing  $e_\Delta$  and the  $c120^\circ$  energy given in (7) rescaled by spin  $S$ . We find  $\alpha_{b2} = \frac{S}{2S+1} \left( \frac{1}{2} + \sqrt{\frac{3S+2}{2}} \right) < \alpha_c$ . Together, the yellow regime in Fig. 3 highlights the parameter space in which we find a dimer ground state. Note that, for our dimer phase diagram, we have only focused on the stability

of the nearest-neighbor dimer state (5). Furthermore, in order to specify an ordered state out of which the dimerized regime might evolve, the classical limit has provided us with a candidate  $c120^\circ$  order. Our analysis does not exclude the possibility that the MLM can host other exotic quantum disordered phases due to its high frustration for  $\alpha < \alpha_c$ . It highlights the nature of the phase transition into the dimerized phase, and possibly additional phase transitions featuring deconfined criticality [32], as a future problem.

It is insightful to compare our dimer phase diagram Fig. 3 with the related scenario in the SSM, for which we have already chosen the appropriate parametrization of (1) in hindsight. We find that the MLM is even more frustrated than the SSM, leading to a stable dimer ground state extending to lower  $\alpha$ : For the isotropic case, the SSM is known to yield  $\alpha_c^{\text{SSM}} \approx 0.74$  [33,34]. Small cluster results from exact diagonalization and the coupled cluster method on a related model to MLM suggest  $\alpha_c$  to be 0.725 [16]. Our larger cluster DMRG calculations, however, indicate an even substantially smaller value  $\alpha_c \approx 0.675$ . The MLM thus sets a new bar of frustration for a 2D model with uniform tilings where an exact dimer ground state appears. In comparison to the SSM, this is rooted in the additional frustration emanating from the red triangles (Fig. 1).

*Conclusions and outlook.* We have introduced the exact dimer ground state solution of the MLM. Aside from the SSM, we find that it is the only other such model in two spatial dimensions with uniform tilings exhibiting such a property. In comparison to the SSM, we find a significantly larger region of stability of the dimer ground state, which is a consequence of the enhanced frustration inherent to the MLM. Magnetic ordering phenomena in the MLM likewise promise highly exotic behavior. This already becomes apparent from the  $c120^\circ$  order in the classical limit, where the canting continuously adjusts to the given bond anisotropy of interactions  $\alpha$ .

The MLM opens up several further theoretical and experimental explorations. First, the stability of the dimer state (5) encourages further investigation within an extended parameter space involving bond and spin exchange anisotropies in (1). Second, by allowing for finite  $B$  in (1), the MLM is expected to show a series of magnetization plateaus and triplet bound states, which promises a phenomenology as rich as the SSM [35–39]. The exact dimer state has a 3-dimer unit cell, whose minimal excitation is a single triplet. Therefore, from this elementary estimate,  $1/3$  and  $2/3$  magnetization plateaus will most certainly appear, complemented by further plateaus resulting from a triplet bound state hierarchy, which is typically located at fractions that are rational multiples of  $1/3$ . This reasoning would already explain the early findings from preliminary exact diagonalization studies in Ref. [16].

There are multiple material realizations of a spin system on the maple-leaf lattice [40–44]. For the MLM,  $\text{MgMn}_3\text{O}_7 \cdot 3\text{H}_2\text{O}$  can be a promising candidate. In general, similar to how the SSM and its experimental realizations have evolved in the past decades, we consider it a fruitful enterprise to reexamine existing maple-leaf compounds and their derivative material families to find new compounds that could host the MLM dimer state. This might be further facilitated by the extremely high frustration of the MLM, as the required minimal bond anisotropy  $2\alpha$  is smaller than for the SSM.

We thank M. Greiter, Y. Iqbal, M. Klett, B. Kumar, R. Moessner, and J. Reuther for illuminating discussions, and, in particular, Y. Iqbal for drawing our attention to the maple-leaf lattice. The work in Würzburg is supported by the Deutsche Forschungsgemeinschaft

(DFG, German Research Foundation) through Project-ID 258499086-SFB 1170 and the Würzburg-Dresden Cluster of Excellence on Complexity and Topology in Quantum Matter—ct.qmat Project-ID 390858490-EXC 2147.

- 
- [1] L. Néel, *Rev. Mod. Phys.* **25**, 58 (1953).
- [2] E. Manousakis, *Rev. Mod. Phys.* **63**, 1 (1991).
- [3] P. A. Lee, N. Nagaosa, and X.-G. Wen, *Rev. Mod. Phys.* **78**, 17 (2006).
- [4] B. S. Shastry and B. Sutherland, *Physica B+C* **108**, 1069 (1981).
- [5] C. K. Majumdar and D. K. Ghosh, *J. Math. Phys.* **10**, 1388 (1969).
- [6] V. Kalmeyer and R. B. Laughlin, *Phys. Rev. Lett.* **59**, 2095 (1987).
- [7] D. F. Schroeter, E. Kapit, R. Thomale, and M. Greiter, *Phys. Rev. Lett.* **99**, 097202 (2007).
- [8] S. A. Kivelson, D. S. Rokhsar, and J. P. Sethna, *Phys. Rev. B* **35**, 8865 (1987).
- [9] R. Moessner and S. L. Sondhi, *Phys. Rev. Lett.* **86**, 1881 (2001).
- [10] X. G. Wen, *Phys. Rev. B* **44**, 2664 (1991).
- [11] X.-G. Wen, *Phys. Rev. B* **65**, 165113 (2002).
- [12] A. Kitaev, *Ann. Phys.* **321**, 2 (2006).
- [13] D. D. Betts, *Proc. N. S. Inst. Sci.* **40**, 95 (1995).
- [14] G. Misguich, C. Lhuillier, B. Bernu, and C. Waldtmann, *Phys. Rev. B* **60**, 1064 (1999).
- [15] D. Schmalfuß, P. Tomczak, J. Schulenburg, and J. Richter, *Phys. Rev. B* **65**, 224405 (2002).
- [16] D. J. J. Farnell, R. Darradi, R. Schmidt, and J. Richter, *Phys. Rev. B* **84**, 104406 (2011).
- [17] R. Makuta and C. Hotta, *Phys. Rev. B* **104**, 224415 (2021).
- [18] I. Affleck, T. Kennedy, E. H. Lieb, and H. Tasaki, *Phys. Rev. Lett.* **59**, 799 (1987).
- [19] D. J. Klein, *J. Phys. A: Math. Gen.* **15**, 661 (1982).
- [20] See Supplemental Material at <http://link.aps.org/supplemental/10.1103/PhysRevB.105.L180412> for the details of the maple-leaf lattice, additional analytic results, details of the classical and DMRG calculations, geometrical analysis of lattices with uniform tiling.
- [21] P. A. McClarty, M. Haque, A. Sen, and J. Richter, *Phys. Rev. B* **102**, 224303 (2020).
- [22] B. Grünbaum and G. C. Shephard, *Math. Mag.* **50**, 227 (1977).
- [23] B. Grünbaum and G. C. Shephard, *Tilings and Patterns* (W. H. Freeman, New York, 1986).
- [24] R. Siddharthan, *Phys. Rev. B* **60**, R9904 (1999).
- [25] K. P. Schmidt and M. Laad, *Phys. Rev. Lett.* **104**, 237201 (2010).
- [26] J. M. Luttinger and L. Tisza, *Phys. Rev.* **70**, 954 (1946).
- [27] T. A. Kaplan and N. Menyuk, *Philos. Mag.* **87**, 3711 (2007).
- [28] J. Schulenburg, J. Richter, and D. Betts, *Acta Phys. Pol., A* **97**, 971 (2000).
- [29] S. V. Isakov, K. Gregor, R. Moessner, and S. L. Sondhi, *Phys. Rev. Lett.* **93**, 167204 (2004).
- [30] J. Herbrych, J. Heverhagen, G. Alvarez, M. Daghofer, A. Moreo, and E. Dagotto, *Proc. Natl. Acad. Sci. USA* **117**, 16226 (2020).
- [31] M. Fishman, S. R. White, and E. M. Stoudenmire, [arXiv:2007.14822](https://arxiv.org/abs/2007.14822).
- [32] T. Senthil, A. Vishwanath, L. Balents, S. Sachdev, and M. P. A. Fisher, *Science* **303**, 1490 (2004).
- [33] P. Corboz and F. Mila, *Phys. Rev. B* **87**, 115144 (2013).
- [34] J. Y. Lee, Y.-Z. You, S. Sachdev, and A. Vishwanath, *Phys. Rev. X* **9**, 041037 (2019).
- [35] T. Momoi and K. Totsuka, *Phys. Rev. B* **61**, 3231 (2000).
- [36] Y. Fukumoto and A. Oguchi, *J. Phys. Soc. Jpn.* **69**, 1286 (2000).
- [37] S. Miyahara, F. Becca, and F. Mila, *Phys. Rev. B* **68**, 024401 (2003).
- [38] J. Dorier, K. P. Schmidt, and F. Mila, *Phys. Rev. Lett.* **101**, 250402 (2008).
- [39] P. Corboz and F. Mila, *Phys. Rev. Lett.* **112**, 147203 (2014).
- [40] D. Cave, F. C. Coomer, E. Molinos, H.-H. Klauss, and P. T. Wood, *Angew. Chem., Int. Ed.* **45**, 803 (2006).
- [41] T. Fennell, J. O. Piatek, R. A. Stephenson, G. J. Nilsen, and H. M. Rønnow, *J. Phys.: Condens. Matter* **23**, 164201 (2011).
- [42] A. Aliev, M. Huvé, S. Colis, M. Colmont, A. Dinia, and O. Mentré, *Angew. Chem., Int. Ed.* **51**, 9393 (2012).
- [43] Y. Haraguchi, A. Matsuo, K. Kindo, and Z. Hiroi, *Phys. Rev. B* **98**, 064412 (2018).
- [44] Y. Haraguchi, A. Matsuo, K. Kindo, and Z. Hiroi, *Phys. Rev. B* **104**, 174439 (2021).